

## Microsphere vs. Microbelt Morphology of Ionic Palladium(II) Complexes

Tae Hwan Noh,<sup>1</sup> In Sung Chun,<sup>1</sup> Young-A Lee,<sup>2</sup> Sungho Ahn,<sup>3</sup>  
Jongki Hong,<sup>3</sup> and Ok-Sang Jung\*<sup>1</sup>

<sup>1</sup>Department of Chemistry, Pusan National University, Pusan 609-735, Korea

<sup>2</sup>Department of Chemistry, Chonbuk National University, Jeonju 561-756, Korea

<sup>3</sup>College of Pharmacy, Kyung Hee University, Seoul 130-701, Korea

Received April 15, 2008; E-mail: oksjung@pusan.ac.kr

A series of palladium(II) complexes containing bis[(4-isonicotinoyloxy)phenyl]sulfide (L), [Pd<sup>II</sup>(L)(tmen)]<sub>2</sub>X<sub>4</sub> (tmen = *N,N,N',N'*-tetramethylethane-1,2-diamine; X = NO<sub>3</sub> and ClO<sub>4</sub>) were prepared and characterized. Reaction of [Pd(tmen)](NO<sub>3</sub>)<sub>2</sub> with L in a mixture of water and acetone affords microspheres whereas reaction of [Pd(tmen)](ClO<sub>4</sub>)<sub>2</sub> with L produces microbelts. The solubility of the products is a significant factor for the formation of morphology. The spherical sizes can be controlled by the evaporation rate of solvents. An array of ≈300 nm and ≈4 μm bimodal spheres was carried out via sonication.

One recent hot issues in supramolecular chemistry is the formation and control of ordered morphology.<sup>1–4</sup> The ability to systematically manipulate micro-sized morphology remains an important goal for functional micro materials such as catalysts, electronic devices, drug-delivery systems, ceramics, pigments, and cosmetics.<sup>5–12</sup> The strategy for controlling such task-specific shapes including spheres, rods, tetrapods, prisms, and cubes is the modification of chemical structures or, alternatively, the change of external condition.<sup>13</sup> Steric effects, surface tension, capillary effects, electric and magnetic forces, van der Waals interaction, hydrophilic interactions, pendent functional groups, and the surfactant/precursor ratio have been applied as driving forces in the formation of artificial morphology.<sup>14–21</sup> When the binding affinity of simple organic/inorganic molecules is sufficiently high, a particle-based morphology is superior to single crystals. A variety of well-defined metal chalcogenide shapes have been produced, but the morphogenesis of discrete metal complexes is rare. Thus, a new, easy method for the morphogenesis of metal complexes, one that does not require any organic additive is highly desired. Moreover, no attention has been focused on the counter anion effects on the formation of ionic metal complexes. To explore the direct counter anion effects on morphology, we report the relevant properties of a uniform morphology formed without the addition of any additives and based on discrete ionic palladium(II) complexes of bis[(4-isonicotinoyloxy)phenyl]sulfide (L). An array of bimodal spheres via sonication was attempted. Such diaminepalladium(II) chemistry might be applicable to various fields such as catalysis,<sup>22</sup> the synthesis of square planar corner building molecules,<sup>23</sup> and the preparation of a magic ring with a “dual character Pd–N bond.”<sup>24</sup>

### Experimental

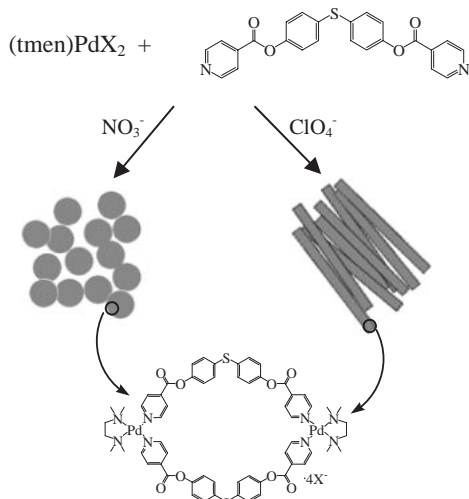
**Materials and Measurements.** [Pd(tmen)](NO<sub>3</sub>)<sub>2</sub> and [Pd(tmen)](ClO<sub>4</sub>)<sub>2</sub> were prepared according to established procedures,<sup>25,26</sup> as was bis[(4-isonicotinoyloxy)phenyl]sulfide (L).<sup>3</sup>

Elemental analysis (C, H, and N) was carried out at the Pusan Center, KBSI, using a Perkin-Elmer 2400 CHNS analyzer. Infrared spectra were obtained in the 4000–400 cm<sup>–1</sup> range on a Perkin-Elmer 16F PC FTIR spectrophotometer, the samples having been prepared as KBr pellets. The <sup>1</sup>H NMR spectra were recorded on a Varian Gemini 300 operating at 300.00 MHz, and the chemical shifts were found to relative to internal SiMe<sub>4</sub>. Thermal analyses were performed under a nitrogen atmosphere at a scan rate of 10 °C min<sup>–1</sup> with a Stanton Red Croft TG 100. Mass spectrometric analysis via fast atom bombardment was performed in chloroform, using a KMS-700 Mstation Mass Spectrometer (Jeol, Japan) and an MS-MP9020D data system. The SEM images were measured on a Hitachi S-4200.

### Preparation of Bis[(4-isonicotinoyloxy)phenyl]sulfide (L).

A chloroform solution (30 mL) of isonicotinoyl chloride hydrochloride (0.06 mol, 10.56 g) was added to a chloroform solution (30 mL) of 4,4'-thiodiphenol (0.03 mol, 6.54 g) and pyridine at 0 °C. The reaction mixture was stirred for 3 h at room temperature. The mixture was quenched with a saturated aqueous K<sub>2</sub>CO<sub>3</sub> solution (50 mL) and extracted with chloroform (3 × 50 mL). The organic layer was dried using MgSO<sub>4</sub>, and the solvent was removed to afford pure L as colorless solid (yield: 92%). Anal. Calcd for C<sub>24</sub>H<sub>16</sub>N<sub>2</sub>O<sub>4</sub>S: C, 67.28; H, 3.76; N, 6.54%. Found: C, 67.21; H, 3.75; N, 6.41%. <sup>1</sup>H NMR (300 MHz, CDCl<sub>3</sub>, SiMe<sub>4</sub>): δ 7.20 (dd, 4H, *J* = 4.8 Hz, *J* = 1.8 Hz), 7.44 (dd, 4H, *J* = 4.5 Hz, *J* = 1.8 Hz), 8.01 (dd, 4H, *J* = 3.0 Hz, *J* = 1.0 Hz), 8.87 (dd, 4H, *J* = 3.0 Hz, *J* = 1.8 Hz). <sup>13</sup>C NMR (125.76 MHz, CDCl<sub>3</sub>, SiMe<sub>4</sub>): δ 163.82, 151.10, 149.95, 136.72, 133.73, 132.58, 123.41, 122.65.

**[Pd(L)(tmen)]<sub>2</sub>(NO<sub>3</sub>)<sub>4</sub>.** L (0.1 mmol, 0.042 g) in 10 mL of acetone was slowly added to an aqueous solution (10 mL) of [Pd(tmen)](NO<sub>3</sub>)<sub>2</sub> (0.1 mmol, 0.035 g). The mixture was stirred for 2 h at room temperature. Evaporation of acetone afforded white spherical product (yield: 70–83%). Slow evaporation for 3 days at ambient temperature produced ≈4 μm diameter microspheres while fast evaporation of acetone for 1 min using a rotary evaporator gave 300 nm diameter submicrospheres. After the product was dried in a vacuum oven for 24 h, elemental analysis



Scheme 1.

was conducted. Anal. Calcd for  $C_{60}H_{64}N_{12}O_{20}Pd_2S_2 \cdot 4H_2O$ : C, 44.42; H, 4.47; N, 10.36%. Found: C, 44.11; H, 4.40; N, 10.21%.  $^1H$ NMR (300 MHz,  $Me_2SO-d_6$ ,  $SiMe_4$ ):  $\delta$  2.61 (s, 12H,  $CH_3$ ), 3.02 (s, 8H,  $CH_2CH_2$ ), 7.29 (d, 8H,  $J = 4.8$  Hz, Ar-H), 7.41 (d, 8H,  $J = 1.8$  Hz, Ar-H), 8.28 (d, 8H,  $J = 4.8$  Hz, Ar-H), 9.47 (d, 8H,  $J = 6.6$  Hz, Ar-H). IR (KBr,  $cm^{-1}$ ): 1748 (s, CO), 1381 (s,  $NO_3^-$ ).

**[Pd(L)(tmen)] $_2$ (ClO $_4$ ) $_4$ .** The same reaction as with L, but with  $[Pd(tmen)](ClO_4)_2$  in place of  $[Pd(tmen)](NO_3)_2$ , produced  $[Pd(L)(tmen)]_2(ClO_4)_4$ . Crystalline microbelts were easily obtained after slow evaporation of acetone at room temperature (yield: 90%). Anal. Calcd for  $C_{60}H_{64}Cl_4N_8O_{24}Pd_2S_2$ : C, 42.39; H, 3.79; N, 6.59%. Found: C, 42.15; H, 3.70; N, 6.69%.  $^1H$ NMR (300 MHz,  $Me_2SO-d_6$ ,  $SiMe_4$ ):  $\delta$  2.60 (s, 12H,  $CH_3$ ), 3.08 (s, 8H,  $CH_2CH_2$ ), 7.29 (d, 8H,  $J = 4.8$  Hz, Ar-H), 7.41 (d, 8H,  $J = 2.1$  Hz, Ar-H), 8.28 (d, 8H,  $J = 4.8$  Hz, Ar-H), 9.47 (d, 8H,  $J = 6.3$  Hz, Ar-H). IR (KBr,  $cm^{-1}$ ): 1748 (s, CO), 1086 (s,  $ClO_4^-$ ). FAB-Mass (matrix: nitrobenzyl alcohol):  $m/z = 1075.0$ ; [Dimer - L -  $HClO_4 - ClO_4$ ] $^+$ , 1173.7; [Dimer - L -  $ClO_4$ ] $^+$ , 1490.5; [Dimer - tmen -  $ClO_4$ ] $^+$ , 1600.5; [Dimer -  $ClO_4$ ] $^+$ .

**Samples for SEM.** The spheres were collected by the filtration using a membrane (membrane filter, Advantec MFS Inc.) for further characterization. The spheres were re-dispersed in distilled water, the suspension was added drop-wise on a glass plate ( $5 \times 5$  mm $^2$ ). The product was dried in a desiccator, and then SEM images of the spheres on the glass plate were taken. The SEM image of the crystalline microbelts,  $[Pd(L)(tmen)]_2(ClO_4)_4$  was measured after the obtained microcrystalline materials were dried.

**Array of Bimodal Spheres in H $_2$ O.** Equimolar microspheres and submicrospheres (10 mg) were sonicated in 10 mL of water at room temperature for 3 min.

## Results and Discussion

**Synthesis.** The ionic palladium(II) complexes,  $[Pd(L)(tmen)]_2(X)_4$ , were prepared by the reaction of an aqueous solution of  $[Pd(tmen)]X_2$  (tmen = *N,N,N',N'*-tetramethylethane-1,2-diamine;  $X^- = NO_3^-$  and  $ClO_4^-$ ) with an acetone solution of L, as shown in Scheme 1. In a typical preparation, L (0.1 mmol) in acetone was added slowly to  $[Pd(tmen)]X_2$  (0.1 mmol) in distilled water. The mixture was refluxed for 2 h, and evaporation of acetone at ambient temperature afforded a white product of  $[Pd(L)(tmen)]_2(X)_4$  in high yield.

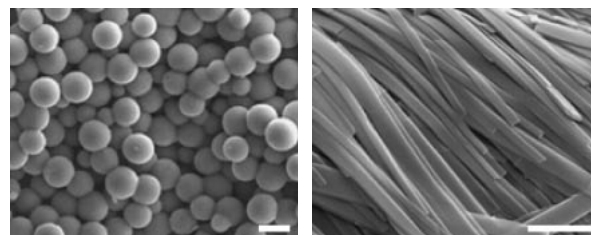
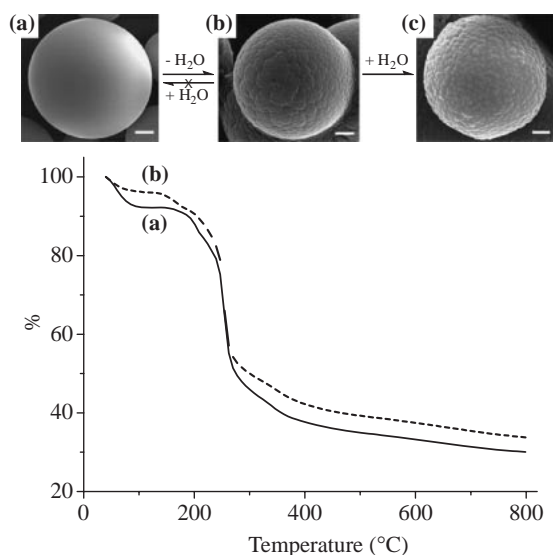


Figure 1. SEM images of microspheres,  $[Pd(L)(tmen)]_2(NO_3)_4$  and microbelts,  $[Pd(L)(tmen)]_2(ClO_4)_4$ . Scale bar: 5  $\mu$ m.

In the case of  $X^- = NO_3^-$ , the reaction yields amorphous microspheres whereas, for  $X^- = ClO_4^-$ , the reaction produces crystalline microbelts. Microspheres of 6–8  $\mu$ m were obtained. The size of the monodisperse spheres could be controlled by the evaporation rate of the solvents. For example, fast evaporation of acetone using a rotary evaporator produces submicrospheres of  $\approx 300$  nm diameters. Thus, slow evaporation of acetone produces larger spheres whereas fast evaporation of acetone affords smaller spheres. The microspheres were collected by filtration using a membrane (membrane filter, Advantec MFS Inc.) for further characterization. The  $^1H$ NMR and IR spectra of both complexes exhibited a similar pattern. The water-solubility of the complexes was not sufficient for measurement of NMR spectra in water. Instead, the  $^1H$ NMR spectrum of  $[Pd(L)(tmen)]_2(NO_3)_4$  in a mixture of water and  $Me_2SO$  (1:1) (2 mM) did not show any catenane phenomenon in the solvent system. The carbonyl peaks of the metal complexes ( $1749$ – $1751$   $cm^{-1}$ ) were blue-shifted relative to that of L ( $1745$   $cm^{-1}$ ). The characteristic anion peaks appeared at  $1382$   $cm^{-1}$  for  $NO_3^-$  and  $1092$   $cm^{-1}$  for  $ClO_4^-$ . In order to measure the molecular weight of the  $[Pd(L)(tmen)]_2(ClO_4)_4$ , the spheres were dissolved in *N,N*-dimethylformamide, and then the solution was mixed with 3-nitrobenzyl alcohol (Sigma, USA) on a FAB probe tip. The molecular weight was determined by the presence of the main fragment peaks and isotope ratios at  $m/z = 1075.0$ ; [Dimer - L -  $HClO_4 - ClO_4$ ] $^+$ , 1173.7; [Dimer - L -  $ClO_4$ ] $^+$ , 1490.5; [Dimer - tmen -  $ClO_4$ ] $^+$ , 1600.5; [Dimer -  $ClO_4$ ] $^+$  (Supporting Information), indicating that the skeletal structure was a cyclodimer consisting of two square-planar palladium(II) units. Both products are stable solids, and soluble in *N,N*-dimethylformamide, dimethylsulfoxide, or a mixture of water and acetone.

**Morphology and Properties.** Scanning electron microscope (SEM) images show that  $[Pd(L)(tmen)]_2(NO_3)_4$  formed microspheres whereas  $[Pd(L)(tmen)]_2(ClO_4)_4$ , under the same conditions, produces microbelts (Figure 1). The microspheres were of regular size (6–8  $\mu$ m diameters) and had smooth surfaces. They contained 8%  $H_2O$  based on thermogravimetric analysis (TGA) data (Figure 2). Only half of the water molecules could be evaporated, even in a vacuum desiccator at  $70^\circ C$  for 24 h. The TGA showed that the spheres are thermally stable up to  $200^\circ C$ . As the water component on the surface was reduced, the surface became cracked. The cracked spheres again absorbed water molecules, but the smooth surface did not return. Such spheres are soluble in water or acetone but only with difficulty, and are most effectively soluble in a mixture (5:5) of water and acetone (Figure 3), indicating that the



**Figure 2.** Process of evaporation ( $a \rightleftharpoons b$ ) and re-adsorption ( $b \rightleftharpoons c$ ) of trace water on the microsphere (top) and thermogravimetric analyses of (a) and (b) microspheres (bottom).

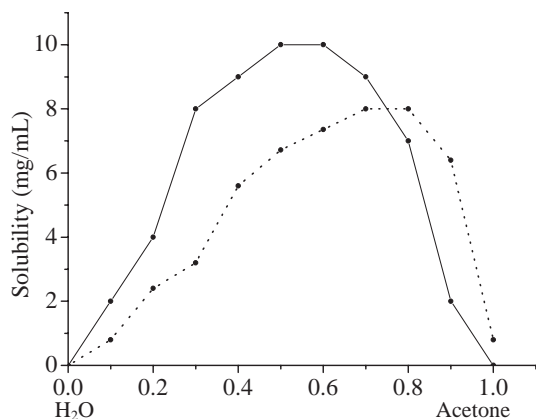


**Figure 3.** Solubility of microspheres,  $[\text{Pd}(\text{L})(\text{tmen})]_2(\text{NO}_3)_4$  (solid line) and microbelts,  $[\text{Pd}(\text{L})(\text{tmen})]_2(\text{ClO}_4)_4$  (dashed line) in mixture of water and acetone.

spheres are typical amphiphilic materials. The crystalline microbelts are best soluble in a mixture (8:2) of water and acetone. The solubility seems to affect to the formation of desirable morphology. In the case of spheres, such an amphiphilic solubility might be a driving force behind the formation of microspherical morphology. The part around the palladium(II) cations and the  $\text{NO}_3^-$  counter anions seems to be hydrophilic, and the L moiety seems to be hydrophobic. Of course, L itself does not show amphiphilic properties or formation of any spherical morphology. The microbelt shapes consisting of  $\text{ClO}_4^-$  complex show a crystalline XRD powder pattern (Supporting Information). Actually, the formation of crystalline microbelts is slower than that of microspheres. According to the TGA data, the microbelts contained almost no water molecules, indicating that  $\text{ClO}_4^-$  is less hydrophilic than  $\text{NO}_3^-$ . In order to quantify the information on surface wettability, the contact angles<sup>3</sup> of a water droplet on the surface of the microspheres and microbelts were measured (Figure 4). The contact angle for the micro-

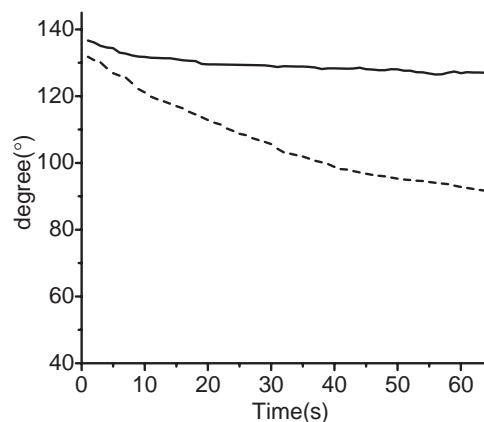


**Figure 4.** Contact angles of a water-droplet on the surfaces of spheres,  $[\text{Pd}(\text{L})(\text{tmen})]_2(\text{ClO}_4)_4$  (solid line) and microbelts,  $[\text{Pd}(\text{L})(\text{tmen})]_2(\text{NO}_3)_4$  (dashed line).

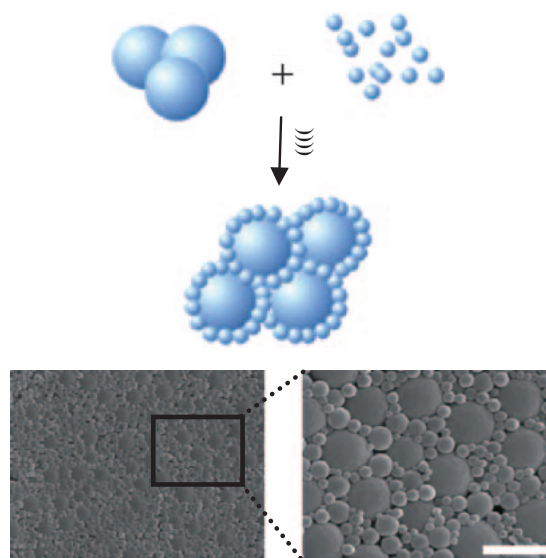


**Figure 5.** Array of bimodal spheres,  $[\text{Pd}(\text{L})(\text{tmen})]_2(\text{NO}_3)_4$  via sonication. Bar = 5  $\mu\text{m}$ .

spheres ( $105^\circ$ ) was smaller than that for the microbelts ( $129^\circ$ ), indicating that the microsphere surfaces are the more hydrophilic. Thus, the wettability of the morphology is strongly dependent on the hydrophilicity of the counter anions. It is worth noting that measuring contact angles is a useful technique for determining quantitative counter anion effects on the hydrophilicity of micro shapes. Such a modulation of surface properties such as wettability, adhesion, and biocompatibility has important implications for both fundamental and technological advances.<sup>27–29</sup> Thus, the contact angles are consistent with a modified Hofmeister series,  $\text{NO}_3^- > \text{ClO}_4^-$ .<sup>30</sup>

For  $[\text{Pd}(\text{L})(\text{tmen})]_2(\text{NO}_3)_4$ , the size of uniform spheres (300 nm–4  $\mu\text{m}$ ) is significantly affected by the evaporation rate of acetone (Figure 5). Slow evaporation of acetone for 3 days at room temperature produces  $\approx 4 \mu\text{m}$  diameter microspheres. Fast evaporation of acetone for 1 min using a rotary evaporator affords  $\approx 300 \text{ nm}$  diameter submicrospheres. As the evaporation rate of acetone increases, the size of spheres decreases. Thus, spheres with medium sizes could be smoothly produced. The packing of bimodal spheres was accomplished in water

suspension by sonication as shown in Figure 5, and indicated the presence of interspherical interactions. Packed bimodal spheres are not easily dissociated in water, presumably owing to the presence of electrostatic interactions between anions and cations<sup>31</sup> on the surfaces of spheres consisting of ionic palladium(II) complexes. This process is an advanced method for reproducibly forming bimodal spheres. As expected, the formation of spheres is fast, whereas the formation of crystalline microbelts is slow. For  $[\text{Pd}(\text{L})(\text{tmen})]_2(\text{NO}_3)_4$ , intermolecular interactions including water molecules as a mediator can be a significant factor in the formation of amorphous spheres. Water molecules on spherical surfaces easily evaporate without imparting any great change to the spherical shape. This easy surface evaporation of water molecules suggests that the water molecules act as mediators, rather than crystallization solvates, in the formation of spheres. Of course, water molecules are essential elements in the formation of spheres. Elemental analysis before and after evaporation of water molecules and  $\nu(\text{OH})$  ( $3300\text{--}3400\text{ cm}^{-1}$ ) indicate the presence and role of water molecules in the formation of the spherical morphology. The complex of an oxidized ligand ( $\text{SO}_2(\text{C}_6\text{H}_4\text{OOC-4-Py})_2$ ) produces hydrogels instead of microspheres. Such a fact indicates that the appropriate hydrophobic properties are another important factor in the formation of spheres. When ethylenediamine was used as a coligand in place of tmen, similar shapes were formed. However, the spheres are easily to aggregate, presumably owing to the presence of interspherical hydrogen bonds. When other counter anions such as  $\text{BF}_4^-$ ,  $\text{CF}_3\text{SO}_3^-$ , and  $\text{PF}_6^-$  were used in place of  $\text{NO}_3^-$ , similar spheres were obtained. We did not observe any significant counter anion effects on the size and shape of the spheres. The exact mechanism is not clear for the formation of the morphologies at this stage. For the formation of the amorphous spheres vs. the crystalline microbelts, the most important factor is solubility in the solvent, that is, the precipitation rate of the solute in the media. Fast precipitation affords amorphous solid. In particular, the formation of sphere is correlated with the amphiphilic properties of the compound. The  $\text{ClO}_4^-$  analogue seems to have a good crystallinity as well as appropriate solubility in the solvent system to form the crystalline microbelts.

### Conclusion

Assembly of ionic metal complexes in an aqueous mixture of solvents was proved to be an effective strategy for the formation of anion-dependent monodisperse morphology. Furthermore, bimodal spheres could be arrayed in aqueous suspension via sonication. This is a rare case of the formation of spherical morphology by means of the concept of ionic metal complexes. The surface wettability of spheres could be extrapolated to the properties of counter anions. The structural modification of metal complexes via their pliability will contribute to the development of micro-based functional materials.

This work was supported by the KOSEF R01-2007-000-20245-0 in Korea.

### Supporting Information

XRD powder patterns of  $[(\text{tmeda})\text{Pd}(\text{L})]_2(\text{NO}_3)_4$  and  $[(\text{tmeda})\text{Pd}(\text{L})]_2(\text{ClO}_4)_4$ . FAB mass of  $[(\text{tmeda})\text{Pd}(\text{L})]_2(\text{ClO}_4)_4$ . SEM

images of  $[(\text{tmeda})\text{Pd}(\text{L})]_2(\text{CF}_3\text{SO}_3)_4$  and  $[(\text{tmeda})\text{Pd}(\text{L})]_2(\text{PF}_6)_4$ .  $^1\text{H}$  NMR spectra of  $[(\text{tmeda})\text{Pd}(\text{L})]_2(\text{NO}_3)_4$  and  $[(\text{tmeda})\text{Pd}(\text{L})]_2(\text{ClO}_4)_4$ . These materials are available free of charge on the web at <http://www.csj.jp/journals/bcsj/>.

### References

- 1 S. Mann, *Angew. Chem., Int. Ed.* **2000**, 39, 3392.
- 2 H. J. Yoon, I. S. Chun, Y. M. Na, Y.-A. Lee, O.-S. Jung, *Chem. Commun.* **2007**, 492.
- 3 I. S. Chun, K. S. Lee, J. Hong, Y. Do, O.-S. Jung, *Chem. Lett.* **2007**, 36, 548.
- 4 I. S. Chun, J. A. Kwon, H. J. Yoon, M. N. Bae, J. Hong, O.-S. Jung, *Angew. Chem., Int. Ed.* **2007**, 46, 4960.
- 5 Y. Xia, P. Yang, Y. Sun, Y. Wu, B. Mayers, B. Gates, Y. Yin, F. Kim, H. Yan, *Adv. Mater.* **2003**, 15, 353.
- 6 B. Liu, H. C. Zeng, *J. Am. Chem. Soc.* **2004**, 126, 8124.
- 7 H. Cölfen, S. Mann, *Angew. Chem., Int. Ed.* **2003**, 42, 2350.
- 8 K. P. Velikov, C. G. Christova, R. P. A. Dullens, A. van Blaaderen, *Science* **2002**, 296, 106.
- 9 X. Sun, Y. Li, *Chem.—Eur. J.* **2003**, 9, 2229.
- 10 M. Li, H. Schnablegger, S. Mann, *Nature* **1999**, 402, 393.
- 11 Q. Peng, Y. Dong, Y. Li, *Angew. Chem., Int. Ed.* **2003**, 42, 3027.
- 12 H. Shi, L. Qi, J. Ma, H. Cheng, *J. Am. Chem. Soc.* **2003**, 125, 3450.
- 13 L. Manna, E. C. Scher, A. P. Alivisatos, *J. Am. Chem. Soc.* **2000**, 122, 12700.
- 14 N. Bowden, A. Terfort, J. Carbeck, G. M. Whitesides, *Science* **1997**, 276, 233.
- 15 D. H. Gracias, J. Tien, T. L. Breen, C. Hsu, G. M. Whitesides, *Science* **2000**, 289, 1170.
- 16 G. M. Whitesides, B. Grzybowski, *Science* **2002**, 295, 2418.
- 17 V. R. Thalladi, G. M. Whitesides, *J. Am. Chem. Soc.* **2002**, 124, 3520.
- 18 N. I. Kovtyukhova, T. E. Mallouk, *Chem.—Eur. J.* **2002**, 8, 4354.
- 19 D. Whang, S. Jin, Y. Wu, C. M. Lieber, *Nano Lett.* **2003**, 3, 1255.
- 20 A. D. Dinsmore, M. F. Hsu, M. G. Nikolaides, M. Marquez, A. R. Bausch, D. A. Weitz, *Science* **2002**, 298, 1006.
- 21 S. Park, J.-H. Lim, S.-W. Chung, C. A. Mirkin, *Science* **2004**, 303, 348.
- 22 Q. Yao, E. P. Kinney, C. Zheng, *Org. Lett.* **2004**, 6, 2997.
- 23 M. Fujita, F. Ibukuro, H. Hagihara, K. Ogura, *Nature* **1994**, 367, 720.
- 24 S. R. Seidel, P. J. Stang, *Acc. Chem. Res.* **2002**, 35, 972.
- 25 Y.-A. Lee, O.-S. Jung, *Angew. Chem., Int. Ed.* **2001**, 40, 3868.
- 26 Y.-A. Lee, K. H. Yoo, O.-S. Jung, *Bull. Chem. Soc. Jpn.* **2003**, 76, 107.
- 27 A. Ulman, *Chem. Rev.* **1996**, 96, 1533.
- 28 R. Colorado, Jr., T. R. Lee, *Langmuir* **2003**, 19, 3288.
- 29 M. K. Chaudhury, G. M. Whitesides, *Science* **1992**, 256, 1539.
- 30 J. W. Lee, E. A. Kim, Y. J. Kim, Y.-A. Lee, Y. Pak, O.-S. Jung, *Inorg. Chem.* **2005**, 44, 3151.
- 31 H. J. Yoon, I. S. Chun, J. P. Kim, Y. S. Lee, O.-S. Jung, *Mater. Lett.* **2008**, 62, 2883.